A Method of Retrieving BRDF from Surface-Reflected Radiance Using Decoupling of Atmospheric Radiative Transfer and Surface Reflection

Alexander Radkevich

Science Systems and Applications, Inc., Hampton, VA 23666, USA; alexander.radkevich@nasa.gov;
Tel.: +1-757-951-1655

check for updates

Abstract: Bi-directional reflection distribution function (BRDF) defines anisotropy of the surface reflection. It is required to specify the boundary condition for radiative transfer (RT) modeling used in aerosol retrievals, cloud retrievals, atmospheric modeling, and other applications. Ground based measurements of reflected radiance draw increasing attention as a source of information about anisotropy of surface reflection. Derivation of BRDF from surface radiance requires atmospheric correction. This study develops a new method of retrieving BRDF on its whole domain, making it immediately suitable for further atmospheric RT modeling applications. The method is based on the integral equation relating surface-reflected radiance, BRDF, and solutions of two auxiliary atmosphere-only RT problems. The method requires kernel-based BRDF. The weights of the kernels are obtained with a quickly converging iterative procedure. RT modeling has to be done only one time before the start of iterative process.

Keywords: BRDF; surface-reflected radiance; ground measurements; atmosphere-surface decoupling

1. Introduction

Radiation reflected from the Earth's surface presents a valuable source of information about surface properties that can be formalized in the bi-directional reflection distribution function (BRDF). That information is required to specify a boundary condition for radiative transfer (RT) modeling, which is used in aerosol retrievals, cloud retrievals, atmospheric modeling, and other applications. Ground based measurements of reflected radiance draw high attention as a source of information about anisotropy of surface reflection [1–7] in the past years, along with development of measurement techniques [8]. Atmospheric correction has to be done to derive BRDF from surface radiance, so retrieval methods were also developed [9,10].

The retrieval methods are based on a comparison of the measured and computed reflected radiance at the ground level. If yet another evaluation of the radiance is needed, then a full radiative transfer problem has to be solved anew for the next estimate of BRDF. Decoupling of the atmospheric radiative transfer and anisotropic surface reflectance allows one to avoid multiple RT computations if standard problems (i.e., no reflection on the boundaries of the atmosphere) are solved. Study by Lyapustin and Knyazikhin [11], the solution was found in the form of a series by the number of reflections. Development in that study was used in the multi-angle implementation of atmospheric correction (MAIAC) [12]. That algorithm uses an approximate expression of the surface-reflected radiance (hereafter, this term is used for radiance reflected by the surface immediately above it), see Equation (2) of that paper. The approximation originates from the necessity to summate the series by the number of reflections. The accuracy of that approximation was found high in Lyapustin and Knyazikhin [11].

Study [13] also presents decoupling of atmospheric RT and surface reflection. Surface-reflected radiance is presented there as a solution of an integral equation relating it with BRDF and radiances transmitted through and reflected by the atmosphere. Solution of that equation provides the informal sum of the series by the number of interactions of a photon with the surface. In this sense, these two techniques are equivalent. Therefore, the necessity to summate a series [11] was replaced by the necessity to solve an integral equation [13]. The approaches to solve that equation if standard problems are solved with the discrete ordinates method and spherical harmonics method were also considered in that study.

A recent study [14] developed yet another method to solve the equation for surface-reflected radiance based on 2D discretization on a unit sphere and iterative solution of the resulting system of linear equations. That paper also considered inversion of the equation for the surface-reflected radiance with respect to BRDF. The resulting equation presents an ill-posed problem, but even if this complication is overcome, it requires knowledge of the reflected radiance on its whole domain, which practically cannot be achieved.

The use of kernel-based BRDF became a standard approach to resolve such a problem [15–17]. Kernel-based BRDF models were used in various terrestrial applications [18–20]. Most of the models are comprised with three kernels though Liu and co-authors presented a five-kernel model [21]. An overview of the modern state of the field is given in Roujean [22]. In particular, that study argued that "the BRDF model matrix is ill-conditioned if the number of kernels would be too much in exceed over three because of their similarity, which leads to linear dependence of model kernels. Therefore, further progress in BRDF modeling and inversion is related to these model extensions and implementation of advanced inversion techniques". One such inversion technique is presented in this paper. Study [22] also states "the kernels could be of any kind of complexity, provided they properly and correctly mimic the observed information", so that selection of kernels for the retrieval model is an important problem that should be addressed based on physical features of the surface. This problem is not considered in this study. The purpose of the development here is to present an algorithm for obtaining kernel weights in a situation when the choice of the kernels is clear.

2. Methodology

2.1. Equation for Surface-Reflected Radiance

If a plane-parallel atmosphere of total optical thickness τ_t and underlain with a surface given by BRDF $\varrho(\mu_1, \mu_2, \phi_1 - \phi_2)$ (please note that both μ_1 and μ_2 are positive here in accordance with bottom boundary condition used in Radkevich [14], see Equation (3) there) is illuminated on its top with monodirectional light making polar angle θ_0 with the vertical axis pointed to the surface, $\mu_0 = \cos(\theta_0)$, then radiance of light reflected by the surface and propagating in direction $(\arccos(-\mu), \phi)$ at the surface level is given by the equation [13]

$$L(\tau = \tau_t, -\mu, \phi, \mu_0) = S(\mu_0, \mu, \phi) + \int_0^{2\pi} d\phi_2 \int_0^1 d\mu_2 K(\mu, \mu_2, \phi - \phi_2) L(\tau = \tau_t, -\mu_2, \phi_2, \mu_0), \quad (1)$$

where source function S and kernel K are given with the expressions

$$S(\mu_0, \mu, \phi) = I_0 \mu_0 \exp(-\tau_t/\mu_0) \rho(\mu_0, \mu, \phi) + \int_0^{2\pi} d\phi_1 \int_0^1 d\mu_1 \, \mu_1 \rho(\mu_1, \mu, \phi - \phi_1) I(\tau = \tau_t, \mu_1, \phi_1, \mu_0), \quad (2)$$

$$K(\mu, \mu_2, \phi - \phi_2) = \int_0^{2\pi} d\phi_1 \int_0^1 d\mu_1 \, \mu_1 \rho(\mu_1, \mu, \phi - \phi_1) J(\tau = 0, -\mu_1, \phi_1 - \phi_2, \mu_2)/I_0, \quad (3)$$

Radiance I in Equation (2) is the solution of the RT problem for the same atmosphere without surface reflection; radiance J in Equation (3) is similar to I but for the atmosphere with inverse order

of layers (flipped-over atmosphere). I_0 is radiance at the top-of-atmosphere level, so that $\mu_0 I_0$ is TOA irradiance.

A recent paper [14] discusses the numerical solution of Equation (1). The key findings that are important in the context of this study are: (1) source function S provides a very good first approximation to the full solution of Equation (1); (2) the use of numerical quadrature with respect to the azimuth variable provides an efficient way to solve the equation without expanding all quantities into Fourier series and consequent summation of the resulting series; and (3) inversion of Equation (1) with respect to BRDF is theoretically possible but does not provide any advantages in retrievals, since it is ill posed and requires knowledge (measurements) of the surface-reflected radiance on its entire domain, which is practically impossible.

2.2. Iterative Fitting Algorithm to Derive BRDF from the Surface-Reflected Radiance

The fact that source function S Equation (2) of Equation (1) provides very good initial approximation of the reflected radiance $L(\tau = \tau_t, -\mu, \phi, \mu_0)$ gives us an idea to improve that initial approximation by iterations. We will assume that the atmospheric state is known, i.e., radiances I and J can be modeled on their entire domains; and that real BRDF can be approximated by a finite set of kernels, see e.g., Lucht, et al, [17],

$$\rho(\theta_s, \theta_v, \phi) \approx \sum_{l=1}^{k} \alpha_l \rho_l(\theta_s, \theta_v, \phi), \tag{4}$$

so that the problem is reduced to obtaining weights of the kernels α_l. We will also assume that BRDF ρ and kernels ρ_l are symmetric functions of relative azimuth ϕ. Then, substituting Equation (4) into Equations (1)–(3) we obtain

$$L(\tau = \tau_t, -\mu, \phi, \mu_0) \approx \sum_{l=1}^{k} \alpha_l \left\{ S_l(\mu_0, \mu, \phi) + \int_0^{2\pi} d\phi_2 \int_0^1 d\mu_2 K_l(\mu, \mu_2, \phi - \phi_2) L(\tau = \tau_t, -\mu_2, \phi_2, \mu_0) \right\}, \tag{5}$$

where

$$S_l(\mu_0, \mu, \phi) = I_0 \mu_0 \exp(-\tau_t/\mu_0) \rho_l(\mu_0, \mu, \phi) + \int_0^{2\pi} d\phi_1 \int_0^1 d\mu_1 \, \mu_1 \rho_l(\mu_1, \mu, \phi - \phi_1) I(\tau = \tau_t, \mu_1, \phi_1, \mu_0), \tag{6}$$

$$K_l(\mu, \mu_2, \phi - \phi_2) = \int_0^{2\pi} d\phi_1 \int_0^1 d\mu_1 \, \mu_1 \rho_l(\mu_1, \mu, \phi - \phi_1) J(\tau = 0, -\mu_1, \phi_1 - \phi_2, \mu_2)/I_0, \tag{7}$$

Surface-reflected radiance L is usually measured on a limited set of sun-to-observer geometries, so we assume that L is known on a sparse set $\{\mu_{0,i}, \mu_i, \phi_i\}$, $i = 1, \dots p$. Then, the algorithm somewhat resembles the iterative process in Gatebe, et at. [23] and BRDF retrievals iterative process of MAIAC [24], see Equation (3) there. Equation (5) is used twice in every step: first to obtain an approximation of BRDF and second to improve current approximation of L.

0-th approximation:

Step A: minimal square fit to find coefficients $\left\{ \alpha_l^{(0)} \right\}$, $l = 1, \dots, k$, so that $\sum_{l=1}^{k} \alpha_l^{(0)} S_l(\mu_0, \mu, \phi)$ is the best match to the set of experimental data $\{L_i\} = \left\{ L(\tau = \tau_t, -\mu_i, \phi_i, \mu_{0,i}) \right\}$;

Step B: compute 0-th approximation of surface-reflected radiance as

$$L(\tau = \tau_t, -\mu, \phi, \mu_0) = \sum_{l=1}^{k} \alpha_l^{(0)} S_l(\mu_0, \mu, \phi). \tag{8}$$

at all values of its arguments needed for evaluation of the integral term in Equation (5);

First approximation:

Step A: minimal square fit to find coefficients $\left\{\alpha_l^{(1)}\right\}$, $l = 1, \ldots, k$, so that

$$\sum_{l=1}^{k} \alpha_l^{(1)} \left\{ S_l(\mu_0, \, \mu, \, \varphi) \, + \, \int_0^{2\pi} d\varphi_2 \int_0^1 d\mu_2 K_l(\mu, \mu_2, \varphi - \varphi_2) L^{(0)}(\tau = \tau_t, -\mu_2, \varphi_2, \mu_0) \right\} \text{ is the best match to}$$

the set of experimental data $\{L_i\}$;

Step B: compute first approximation of surface-reflected radiance as

$$L^{(1)}(\tau = \tau_t, -\mu, \varphi, \mu_0) = \sum_{l=1}^{k} \alpha_l^{(1)} \left\{ S_l(\mu_0, \, \mu, \, \varphi) \, + \, \int_0^{2\pi} d\varphi_2 \int_0^1 d\mu_2 K_l(\mu, \mu_2, \varphi - \varphi_2) L^{(0)}(\tau = \tau_t, -\mu_2, \varphi_2, \mu_0) \right\}, \tag{9}$$

at all values of its arguments needed to evaluate the integral term in Equation (5). The steps of the first approximation can be repeated until desirable convergence is reached.

2.3. Numerical Consideration

Due to the assumption that all quantities in the equations above are symmetric functions of azimuth, all integrations over interval $[0, 2\pi]$ can be reduced to integration over interval $[0, \pi]$. This study employs the same quadrature scheme as used in Radkevich [14]: Gaussian rule $\{\mu_j, \beta_j\}$, $j = 1, \ldots, m$ on $[0, 1]$ and trapezoidal rule on a regular grid on $[0, \pi]$ $\{\varphi_i, w_i\}$, $i = 1, \ldots, n$, $\varphi_i = \Delta\varphi(i-1)$, $w_i = \Delta\varphi(1 - \delta_{i,0}/2 - \delta_{i,n}/2)$, $\Delta\varphi = \pi/(n-1)$. Discretized Equation (1) takes the form

$$L_{j,i} = S_{j,i} + \sum_{s=1}^{m} \sum_{l=1}^{n} K_{j,i,s,l} L_{s,l}; \quad L_{j,i} = L(\tau = \tau_t, -\mu_j, \varphi_i, \mu_0); \quad i = 1, \ldots, n; \quad j = 1, \ldots, m; \tag{10}$$

where

$$S_{j,i} = S(\mu_0, \mu_j, \varphi_i); \tag{11}$$

$$K_{j,i,s,l} = \beta_j w_i \left(\left\{ \begin{array}{l} K\left(\mu_j, \mu_s, \varphi_{i-l+1}\right), \, 1 \leq l \leq i \\ K\left(\mu_j, \mu_s, \varphi_{l-i+1}\right), \, i+1 \leq l \leq n \end{array} \right\} + \left\{ \begin{array}{l} K\left(\mu_j, \mu_s, \varphi_{i+l-1}\right), \, 1 \leq l \leq n-i+1 \\ K\left(\mu_j, \mu_s, \varphi_{2n-i-l+1}\right), \, n-i+2 \leq l \leq n \end{array} \right\} \right), \tag{12}$$

Numerical tests of the performance of the suggested algorithm were conducted with the following atmospheric conditions: the atmosphere is a uniform layer comprised of (a) Rayleigh scattering and weak gas absorption, so that single scattering albedo (SSA) is 0.999 and optical thickness τ_R of 0.1 (this roughly corresponds to the wavelength of 550 nm) and (b) transported mineral dust aerosol from OPAC [25] with optical thicknesses τ_A of 0.1, 0.5, and 1.0. Therefore, simplified atmospheric conditions are defined with Rayleigh scattering, aerosol scattering and absorption of a known aerosol type, and weak gas absorption. Single scattering properties of aerosol were computed with code SPHER [26]. It was found that it is essential to retain 138 terms in Legendre expansion of the phase function of the selected type of aerosol. Radiances L, I, J were computed with DISORT using 158 streams for all μ_0 and μ being nodes of the Gaussian quadrature of order $m = 24$ and φ on the regular grid described above with $n = 49$.

Surface-reflected radiance was computed for two BRDF models. First, bare soil model by Nilson and Kuusk [27], see Equations (11) and (11′) there

$$\rho(\theta_s, \theta_v, \varphi) = a\left(b_0 + b_1\theta_s\theta_v\cos\varphi + b_2\left(\theta_s^2 + \theta_v^2\right) + b_3\theta_s^2\theta_v^2\right)$$
$$a = \lim_{\theta_s \to \pi/2} a(\theta_s) = 0.2; \quad b_0 = 0.31489; \quad b_1 = 0.14129; \quad b_2 = -0.082511; \quad b_3 = 0.14779 \tag{13}$$

The second model is MODIS BRDF, see Equations (37)–(44) [17]

$$\rho(\theta_s, \theta_v, \varphi) = \frac{1}{\pi}\left(f_{iso} + f_{vol}K_{vol}(\theta_s, \theta_v, \varphi) + f_{geo}K_{geo}(\theta_s, \theta_v, \varphi)\right), \tag{14}$$

where factor $1/\pi$ comes in due to the difference in definitions, so that we will denote $\alpha_1 = f_{iso}/\pi$, $\alpha_2 = f_{vol}/\pi$, $\alpha_3 = f_{geo}/\pi$. In this study, the following particular values of the parameters were used: $f_{iso} = 0.265$, $f_{vol} = 0.066$, $f_{geo} = 0.000$ ($\alpha_1 = 0.08435$, $\alpha_2 = 0.02101$, $\alpha_3 = 0.0000$) representing actual MODIS BRDF retrievals [28] over the Sahara Desert.

3. Results of BRDF Retrievals

Surface-reflected radiance *L*, obtained by solving the boundary value problem to the radiative transfer equation with DISORT, can be used as a simulation of experimental measurements if taken at sparse geometries. Paper [14] compares radiance *L* directly computed with DISORT with numerical solution of Equation (1) using radiance *I* and *J* also computed with DISORT. It was found that the solution obtained with DISORT has noticeable azimuthal noise of the order of few percent, see Figures 1–3 there. The numerical solution of Equation (1) obtained in Radkevich [14] is not independent from errors introduced by DISORT, thus it cannot be considered as more accurate. Though the origin of this noise is beyond the scope of this paper, its presence in the solution makes it a valuable opportunity to check robustness of BRDF retrievals by the iterative process described above.

Numerical experiments below will use surface-reflected radiance *L* computed on the grid described in Section 2.3. Random selections of 12 and 60 geometries, i.e., values of $\{\mu_{0,i}, \mu_i, \phi_i\}$, were performed for each optical thickness, so that retrievals were performed on different sets of data. The purpose of this study is to test the developed algorithm, so the optimized selection of data samples suggested in study [29] was not used. The final results of retrievals are summarized in Tables 1 and 2. The iterative process of retrievals are shown in Figures 1–3. As one can see from the figure's zeroth iteration, Equation (8) provides good accuracy but it can be improved with the first iteration, Equation (9). The difference between first and second iterations can be hardly seen on the graphs. Within an accuracy of seven decimal figures, there is no difference between the second and all subsequent iterations. Therefore, for practical purposes zeroth and first iterations are enough for the process to converge.

Table 1a,b show that the increase of the aerosol optical thickness from 0.1 to 0.5 causes the increase of the standard deviation σ_l of the retrieved parameters α_l while further increase of τ_A to 1.0 does not cause the same effect. Table 2a,b also show no clear tendency for σ_l in this case. Also, greater τ_A (and, consequently, greater τ_t) leads to greater difference between $\overline{\alpha}_l$ and theoretical values $\alpha_{t,l}$ in some cases. However, theoretical values $\alpha_{t,l}$ either falls into 1-σ confidence interval around the mean values $\overline{\alpha}_l$ or the relative difference between $\overline{\alpha}_l$ and $\alpha_{t,l}$ does not exceed 2%.

Table 1. Parameters of Nilson–Kuusk BRDF, Equation (13), retrieved from surface radiance using 10 sets of 60 (a), and 10 sets of 12 (b) randomly selected sun-to-sensor geometries for different optical thickness of the atmosphere multiplied by 100.

Parameter	Theoretical Value	$\tau_t = 0.2$: $\tau_R = 0.1, \tau_A = 0.1$		$\tau_t = 0.6$: $\tau_R = 0.1, \tau_A = 0.5$		$\tau_t = 1.1$: $\tau_R = 0.1, \tau_A = 1.0$	
		Mean Value	Standard Deviation	Mean Value	Standard Deviation	Mean Value	Standard Deviation
(a)							
α_1	6.298	6.286	0.004	6.260	0.015	6.243	0.008
α_2	2.826	2.815	0.008	2.793	0.027	2.809	0.033
α_3	−1.650	−1.646	0.004	−1.645	0.019	−1.637	0.017
α_4	2.956	2.948	0.013	2.964	0.055	2.953	0.061
(b)							
α_1	6.298	6.291	0.026	6.256	0.109	6.193	0.325
α_2	2.826	2.805	0.024	2.866	0.141	2.770	0.160
α_3	−1.650	−1.656	0.045	−1.622	0.195	−1.564	0.314
α_4	2.956	2.968	0.091	2.933	0.297	2.860	0.323

Table 2. Parameters of MODIS BRDF, Equation (14), retrieved from surface radiance using 10 sets of 60 (a), and 10 sets of 12 (b) randomly selected sun-to-sensor geometries for different optical thickness of the atmosphere multiplied by 100.

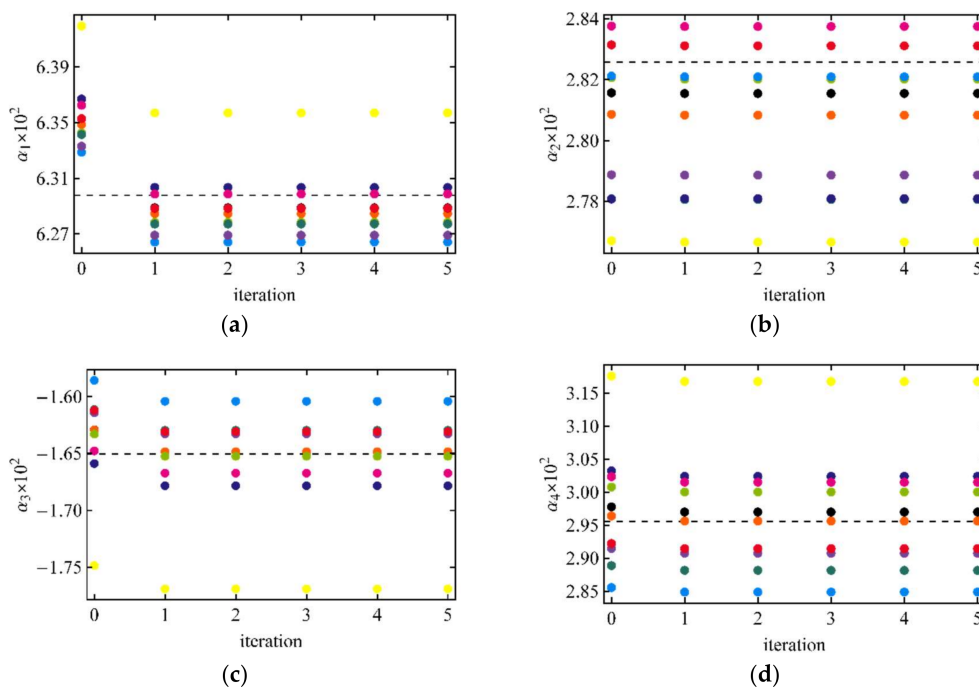|		$\tau_t = 0.6$: $\tau_R = 0.1, \tau_A = 0.5$		$\tau_t = 1.1$: $\tau_R = 0.1, \tau_A = 1.0$	
Parameter	Theoretical Value	Mean Value	Standard Deviation	Mean Value	Standard Deviation
		(a)			
α_1	8.435	8.392	0.012	8.373	0.016
α_2	2.101	2.156	0.072	2.099	0.058
α_3	0.	0.005	0.008	-0.001	0.005
		(b)			
α_1	8.435	8.348	0.079	8.404	0.086
α_2	2.101	2.163	0.171	2.187	0.146
α_3	0.	-0.026	0.060	0.012	0.043

(a)

(b)

(c)

(d)

Figure 1. Convergence of coefficients α_l ($\times 100$) in the case of BRDF (Equation (13)) with $\tau_R = 0.1$, $\tau_R = 0.1$. Different colors are 10 random realizations of 12 observations. Dashed lines—theoretical values. (**a**) α_1; (**b**) α_2; (**c**) α_3; (**d**) α_4.
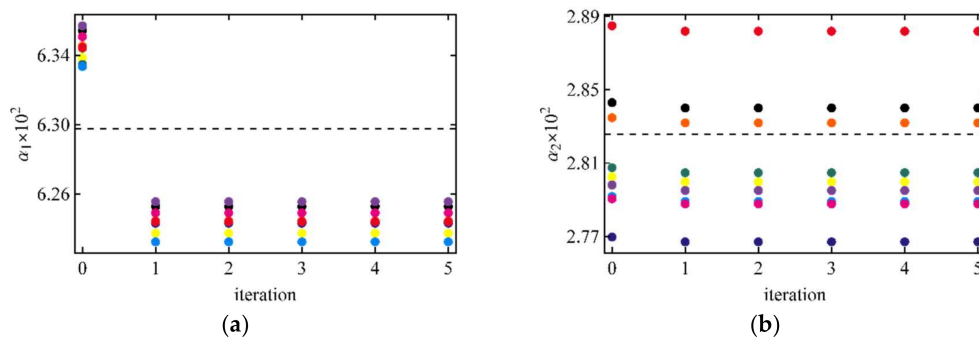

(a)

(b)

Figure 2. *Cont.*
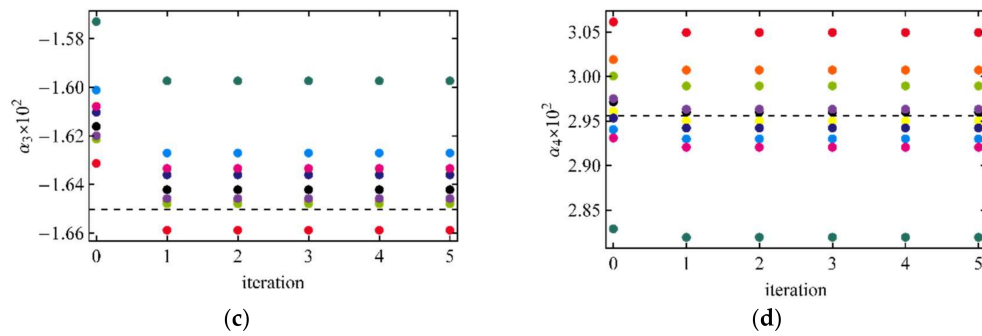
Figure 2. The same as Figure 1 but with $\tau_A = 1.0$ and for 10 random realizations of 60 observations. (**a**) α_1; (**b**) α_2; (**c**) α_3; (**d**) α_4.
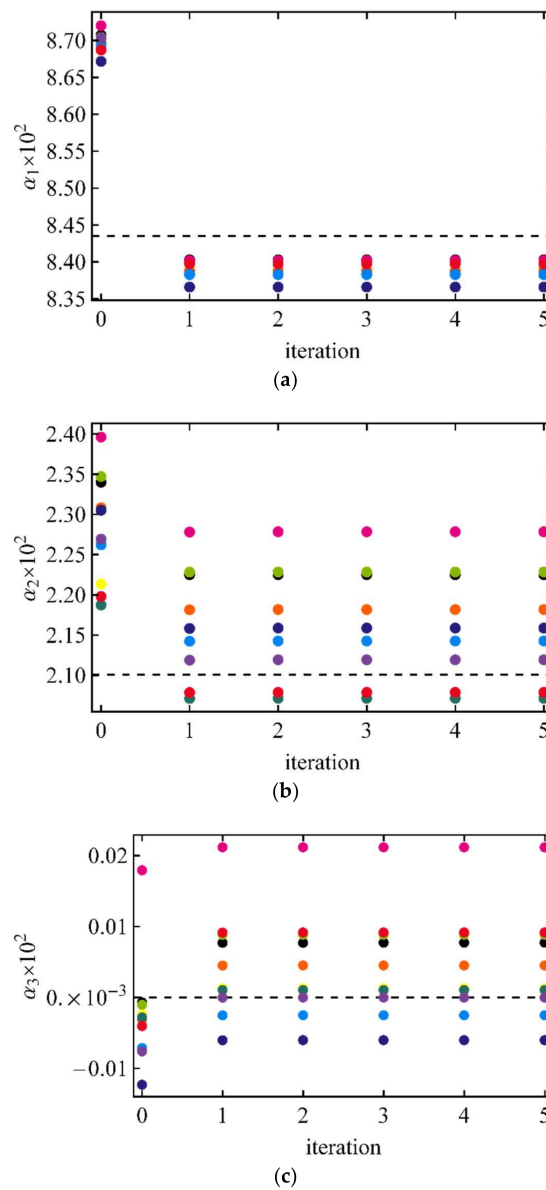

Figure 3. Convergence of coefficients α_l ($\times 100$) in the case of BRDF (Equation (14)) with $\tau_R = 0.1$, $\tau_R = 0.5$. Different colors are 10 random realizations of 60 observations. Dashed lines—theoretical values. (**a**) α_1; (**b**) α_2; (**c**) α_3.

4. Discussion

Analysis of Tables 1 and 2 shows that mean values over 10 randomly selected sun-to-sensor geometries are closer to theoretical values for optically thin atmosphere. It means that even in the ideal case of modeling surface signals with known BRDF and atmospheric conditions, the accuracy of the radiative transfer modeling affects the accuracy of BRDF retrievals. The problem here is at least two-fold. First, the noise in surface-reflected radiance increases with the increase of the optical thickness, making retrievals from it less accurate. Second, since the retrieval process depends on the radiances *I* and *J* transmitted through and reflected by unbound atmosphere, their accuracy and potential presence of noise also affect the accuracy of the retrieval process.

The iterative process itself shows very quick convergence regardless of the surface type and atmospheric conditions.

The accuracy of the retrievals under different atmospheric conditions and for different surfaces can be illustrated with 1-σ confidence intervals relative to the theoretical value for those parameters which have non-zero $\alpha_{t,l}$

$$\varepsilon_\pm = [(|\bar{\alpha}_l| \pm \sigma_l)/|\alpha_{t,l}| - 1] \times 100\%, \tag{15}$$

These relative intervals are presented in Tables 3 and 4 below.

Table 3. Relative confidence intervals, Equation (15), of the retrieved parameters of Nilson–Kuusk BRDF, Equation (13), retrieved from surface radiance using 10 sets of 60 (a), and 10 sets of 12 (b) randomly selected sun-to-sensor geometries for different optical thickness of the atmosphere.

	$\tau_t = 0.2$: $\tau_R = 0.1, \tau_A = 0.1$		$\tau_t = 0.6$: $\tau_R = 0.1, \tau_A = 0.5$		$\tau_t = 1.1$: $\tau_R = 0.1, \tau_A = 1.0$	
	ϵ_-	ϵ_+	ϵ_-	ϵ_+	ϵ_-	ϵ_+
			(a)			
α_1	−0.25	−0.13	−0.84	−0.37	−1.00	−0.75
α_2	−0.67	−0.11	−2.12	−0.21	−1.77	0.57
α_3	−0.48	0.00	−1.45	0.85	−1.82	0.24
α_4	−0.71	0.17	−1.59	2.13	−2.17	1.96
			(b)			
α_1	−0.52	0.30	−2.40	1.06	−6.83	3.49
α_2	−1.59	0.11	−3.57	6.40	−7.64	3.68
α_3	−2.36	3.09	−13.52	10.12	−24.24	13.82
α_4	−2.67	3.48	−10.83	9.27	−14.17	7.68

Table 4. Relative confidence intervals, Equation (15), of the retrieved parameters of MODIS BRDF, Equation (14), retrieved from surface radiance using 10 sets of 60 (a), and 10 sets of 12 (b) randomly selected sun-to-sensor geometries for different optical thickness of the atmosphere.

	$\tau_t = 0.6$: $\tau_R = 0.1, \tau_A = 0.5$		$\tau_t = 1.1$: $\tau_R = 0.1, \tau_A = 1.0$	
	ϵ_-	ϵ_+	ϵ_-	ϵ_+
		(a)		
α_1	−0.65	−0.37	−0.92	−0.55
α_2	−0.81	6.04	−2.86	2.67
		(b)		
α_1	−1.97	−0.09	−1.39	0.65
α_2	−5.19	11.09	−2.86	11.04

Confidence intervals are generally smaller for smaller optical thicknesses and for the greater number of 'observations' used in the retrieval process. It is easy to see that, in many instances, one parameter has positive bias while another has negative. This leads to some cancellation of errors, reducing the overall error in albedo.

It is important to mention that for MODIS BRDF (Equation (14)) retrieval testing one of the parameters, α_3, was deliberately chosen to be zero. The purpose was to check how accurately this zero can be caught by the retrieval algorithm. Lucht and co-authors [17] argued that retrieved parameters of BRDF (Equation (14)) should be non-negative. Lewis [16], considering retrievals of the kernel weight with minimization of the error function, argued that "the minimum of the error function described above can sometimes lie outside of physical limits. In this case, the minimum lies on one of the constraint boundaries in N_k-dimensional space." (N_k is the number of kernels, *k* in notation of this paper). Following this idea, study [17] suggests that "if the mathematical inversion produces a negative parameter, the next best valid value for this parameter is zero, under which imposed condition, the remaining kernel parameters should be re-derived." In the case presented in Figure 3c, all retrievals are wrong, both positive and negative. There are three negative and seven positive retrievals there. Following the approach above, negative values should be set to zero and the retrieval algorithm should be re-run without a third kernel while sevrn positive but equally wrong values should be left as is. The approach can be modified in this situation. If an algorithm is intended to be used on a certain amount of data points of certain quality, then performance (absolute error δ_l of each parameter) of the retrievals can be established statistically with extensive radiative transfer modeling. Then, if a retrieved value α_l falls into an interval $\alpha_{m,l} \pm \delta_l$ around its marginal value $\alpha_{m,l}$, α_l should be set $\alpha_{m,l}$. In the case shown in Figure 3c $\alpha_{m,3} = 0.0$, δ_3 can be set—e.g., equal $\sigma_3 = 0.008$—see the corresponding value in Table 2a. This eliminates four (out of seven) positive values of α_3. Setting $\delta_3 = 2\sigma_3$ eliminates six and $\delta_3 = 3\sigma_3$ eliminates all seven positive (and wrong) retrievals of α_3.

5. Conclusions

An algorithm for retrievals of BRDF from the surface-reflected radiance measured at the ground level is presented. The algorithm is based on the equation relating BRDF with the surface-reflected radiance and the solutions of the RT problems for unbound atmosphere. The previous analysis of the contributions of the different terms of the equation for the reflected radiance suggested that only minor correction to the source term of the equation has to be done. Therefore, fast convergence of the iterative process could be expected.

The presented algorithm requires an assumption on the atmospheric condition. It is based on kernel-based BRDF; therefore, it also requires an assumption on the functional form of the kernels comprising BRDF. The algorithm returns the weights of the kernels. The choice of the kernels depends on the physical properties of the surface. A potential application of the algorithm is derivation of BRDF parameter from measurements acquired in ground-based experimental campaigns. It is desirable to have measurements performed simultaneously with sun-photometer measurements similar to AERONET [30] to ensure accurate retrieval of aerosol properties.

It was shown that the algorithm converges very quickly; no more than one iteration (after initial guess) is needed. Accuracy of the algorithm depends on the number of experimental measurements used for retrievals, optical thickness of the atmosphere, and the quality of the measurements of the surface-reflected radiance. The last two factors may not be independent in the context of this study since the surface-reflected radiance was simulated with DISORT. It was shown in a previous study [14] that there is some noise in those simulations with magnitude increasing with the optical thickness of the atmosphere. Retrievals were performed on the sets of 12 and 60 randomly selected sun-to-sensor geometries. While the mean values of the retrieved kernel weights over 10 sets of geometries are within ~5% of the theoretical values for both 12 and 60 samples (with better matches for optically thinner cases), the range on those sets are wider for the smaller number reaching up to ~25% in certain cases, but staying generally within ~10%.

References

1. Meister, G.; Wiemker, R.; Bienlein, J. In Situ BRDF Measurements of Selected Surface Materials to Improve Analysis of Remotely Sensed Multispectral Imagery. *ISPRS Arch.* **1996**, *31 Pt B7*, 493–498.

2. Deering, D.W.; Eck, T.F.; Grier, T. Shinnery Oak Bidirectional Reflectance Properties and Canopy Model Inversion. *IEEE Trans. Geosci. Remote Sens.* **1992**, *30*, 339–348. [CrossRef]

3. Leroux, C.; Deuzé, J.-L.; Goloub, P.; Sergent, C.; Fily, M. Ground measurements of the polarized bidirectional reflectance of snow in the near-infrared spectral domain: Comparison with model results. *J. Geophys. Res.* **1998**, *103*, 19721–19731. [CrossRef]

4. Hudson, S.R.; Warren, S.G.; Brandt, R.E.; Grenfell, T.C.; Six, D. Spectral bidirectional reflectance of Antarctic snow: Measurements and parameterization. *J. Geophys. Res.* **2006**, *111*, D18106. [CrossRef]

5. Huang, X.; Jiao, Z.; Dong, Y.; Zhang, H.; Li, X. Analysis of BRDF and Albedo Retrieved by Kernel-Driven Models Using Field Measurements. *IEEE J. Sel. Top. Appl. Earth Obs. Remote Sens.* **2013**, *6*, 149–161. [CrossRef]

6. Chopping, M.J. Testing a LiSK BRDF Model with in Situ Bidirectional Reflectance Factor Measurements over Semiarid Grasslands. *Remote Sens. Environ.* **2000**, *74*, 287–312. [CrossRef]

7. Walthall, C.; Roujean, J.-L.; Morisette, J. Field and landscape BRDF optical wavelength measurements: Experience, techniques and the future. *Remote Sens. Rev.* **2000**, *18*, 503–531. [CrossRef]

8. Bruegge, C.; Helmlinger, M.; Conel, J.; Gaitley, B.; Abdou, W. PARABOLA III—A sphere-scanning radiometer for field determination of surface anisotropic reflectance functions. *Remote Sens. Rev.* **2000**, *19*, 75–94. [CrossRef]

9. Martonchik, J.V. Retrieval of surface directional reflectance properties using ground level multiangle measurements. *Remote Sens. Environ.* **1994**, *50*, 303–316. [CrossRef]

10. Lyapustin, A.I.; Privette, J.L. A new method of retrieving surface bidirectional reflectance from ground measurements: Atmospheric sensitivity study. *J. Geophys Res.* **1999**, *104*, 6257–6268. [CrossRef]

11. Lyapustin, A.I.; Knyazikhin, Y. Green's function method for the radiative transfer problem. I. Homogeneous non-Lambertian surface. *Appl. Opt.* **2001**, *40*, 3495–3501. [CrossRef] [PubMed]

12. Lyapustin, A.; Martonchik, J.; Wang, Y.; Laszlo, I.; Korkin, S. Multi-Angle Implementation of Atmospheric Correction (MAIAC): Part 1. Radiative Transfer Basis and Look-Up Tables. *J. Geophys. Res.* **2011**, *116*, D03210. [CrossRef]

13. Radkevich, A. A new look at decoupling of atmospheric radiative transfer and anisotropic surface reflection. *JQSRT* **2013**, *127*, 140–148. [CrossRef]

14. Radkevich, A. Iterative discrete ordinates solution of the equation for surface-reflected radiance. *JQSRT* **2017**, *202*, 114–125. [CrossRef]

15. Roujean, J.-L.; Leroy, M.; Deschamps, P.Y. A bidirectional reflectance model of the Earth's surface for the correction of remote sensing data. *J. Geophys. Res.* **1992**, *97*, 20455–20468. [CrossRef]

16. Lewis, P. The utility of kernel-driven BRDF models in global BRDF and albedo studies. In Proceedings of the Geoscience and Remote Sensing Symposium, Firenze, Italy, 10–14 July 1995. [CrossRef]

17. Lucht, W.; Schaaf, C.B.; Strahler, A.H. An algorithm for the retrieval of albedo from space using semiempirical BRDF models. *IEEE Trans. Geosci. Remote Sens.* **2000**, *38*, 977–998. [CrossRef]

18. Pokrovsky, O.; Roujean, J.-L. Land surface albedo retrieval via kernel-based BRDF modeling: I. Statistical inversion method and model comparison. *Remote Sens. Environ.* **2002**, *84*, 100–119. [CrossRef]

19. Gao, F.; Schaaf, C.B.; Strahler, A.H.; Jin, Y.; Li, X. Detecting vegetation structure using a kernel-based BRDF model. *Remote Sens. Environ.* **2003**, *86*, 198–205. [CrossRef]

20. Román, M.O.; Gatebe, C.K.; Schaaf, C.B.; Poudyal, R.; Wang, Z.; King, M.D. Variability in surface BRDF at different spatial scales (30 m–500 m) over a mixed agricultural landscape as retrieved from airborne and satellite spectral measurements. *Remote Sens. Environ.* **2011**, *115*, 2184–2203. [CrossRef]

21. Liu, S.; Liu, Q.; Liu, Q.; Wen, J.; Li, X. The Angular and Spectral Kernel Model for BRDF and Albedo Retrieval. *IEEE J. Sel. Top. Appl. Earth Obs. Remote Sens.* **2010**, *3*, 242–256. [CrossRef]

22. Roujean, J.-L. Inversion of Lumped Parameters Using BRDF Kernels. *Compre Remote Sens.* **2018**, *3*, 23–34. [CrossRef]

23. Gatebe, C.K.; King, M.D.; Lyapustin, A.I.; Arnold, G.T.; Redemann, J. Airborne Spectral Measurements of Ocean Directional Reflectance. *J. Atmos. Sci.* **2005**, *62*, 1072–1092. [CrossRef]

24. Lyapustin, A.I.; Wang, Y.; Laszlo, I.; Hilker, T.; Hall, F.G.; Sellers, P.J.; Tucker, C.J.; Korkin, S.V. Multi-angle implementation of atmospheric correction for MODIS (MAIAC): 3. Atmospheric correction. *Remote Sens. Environ.* **2012**, *127*, 385–393. [CrossRef]

25. Hess, M.; Koepke, P.; Schult, I. Optical Properties of Aerosols and Clouds: The Software Package OPAC. *BAMS* **1998**, *79*, 831–844. [CrossRef]

26. Mishchenko, M.I.; Travis, L.D.; Lacis, A.A. *Scattering, Absorption, and Emission of Light by Small Particles*; Cambridge University Press: Cambridge, UK, 2002; 448p, ISBN 9780521782524.

27. Nilson, T.; Kuusk, A. A reflectance model for the homogeneous plant canopy and its inversion. *Remote Sens. Environ.* **1989**, *27*, 157–167. [CrossRef]

28. Schaaf, C.B.; Gao, F.; Strahler, A.H.; Lucht, W.; Li, X.; Tsang, T.; Strugnell, N.C.; Zhang, X.; Jin, Y.; Muller, J.-P.; et al. First Operational BRDF, Albedo and Nadir Reflectance Products from MODIS. *Remote Sens. Environ.* **2002**, *83*, 135–148. [CrossRef]

29. Pokrovsky, O.; Roujean, J.-L. Land surface albedo retrieval via kernel-based BRDF modeling: II. An optimal design scheme for the angular sampling. *Remote Sens. Environ.* **2002**, *84*, 120–142. [CrossRef]

30. Holben, B.N.; Eck, T.F.; Slutsker, I.; Tanre, D.; Buis, J.P.; Setzer, A.; Vermote, E.; Reagan, J.A.; Kaufman, Y.; Nakajima, T.; et al. AERONET—A federated instrument network and data archive for aerosol characterization. *Remote Sens. Environ.* **1998**, *66*, 1–16. [CrossRef]